

Photosensitive Polynorbornene Based Dielectric. II. Sensitivity and Spatial Resolution

Yiqun Bai,¹ Punit Chiniwalla,¹ Edmund Elce,² Sue Ann Bidstrup Allen,¹ Paul A. Kohl¹

¹*School of Chemical Engineering, Georgia Institute of Technology, Atlanta, Georgia 30332-0100*

²*Promerus LLC, 9921 Brecksville Road, Brecksville, Ohio 44141*

Received 10 March 2003; revised 1 May 2003; accepted 14 September 2003

ABSTRACT: Photodefinable poly(decylnorbornene-*co*-epoxidenorbornene) copolymer has been developed as a dielectric material for electronic packaging applications. The photodefinition properties of the polymer are affected by the copolymer composition, the concentration of photoactive compound and the process conditions. In particular, ultra-high contrast conditions were found to promote the fabrication of vertical sidewall structures. For photodefined structures, the vertical sidewalls were obtained at specific formulations and process conditions. Under different conditions, non-vertical features were observed. Rutherford backscattering analysis (RBS), X-ray photoelectron spectroscopy (XPS), Fourier transform infrared spectroscopy (FTIR), and scanning electron microscopy (SEM) were used to study the

photodefinition properties. In this article, a mechanism based on the diffusion of photoactive compounds from the exposed area to the unexposed area is presented. The transport of photoactive compounds takes place through the free volume that results from solvent evaporation. The diffusion of the photoactive compounds to the surface of the polymer film results in a higher concentration of photogenerated acid at the surface. The movement of the photoactive compounds occurs in both the in-plane and through-plane directions. © 2004 Wiley Periodicals, Inc. *J Appl Polym Sci* 91: 3031–3039, 2004

Key words: crosslinking; dielectric properties; photopolymerization

INTRODUCTION

Advances in electronic systems require devices with higher speed, higher packing density, and higher functionality. Interconnect delay can be improved by using more conductive metals and insulators with lower dielectric constants. For example, photosensitive polymers have attracted interest for low dielectric constant applications because they can be patterned directly by using standard photolithography techniques, which simplifies the process steps and makes integration easier.¹ Via-holes formed in the dielectric film can have sloped or vertical (straight) sidewalls. Sloped sidewalls have specific uses, such as the conformal coverage of metals. Vertical sidewalls are valuable in high spatial resolution applications, such as plating molds (e.g. Damascene processes) and as vertical waveguides.

A new polynorbornene-based (PNB) photosensitive dielectric polymer (Avatrel™) has been introduced for packaging applications. In this polymer system, decyl side groups on the PNB polymer have been shown to improve its mechanical properties by lowering the modulus and increasing the elongation at break. Epoxide side groups are added to provide crosslinkable sites. In the poly(decylnorbornene-*co*-epoxidenor-

bornene) copolymer, decylnorbornene (decylNB), and epoxidenorbornene (epoxideNB) are randomly polymerized to form copolymers. The chemical structure of polynorbornene is shown in Figure 1.

Poly(decylNB-*co*-epoxideNB) has a low dielectric constant, modulus, and residual stress. The ability to photodefine structures simplifies the processing procedure. In this article, the photochemistry of formulated poly(decylNB-*co*-epoxideNB) is described. Rutherford backscattering analysis (RBS), X-ray photoelectron spectroscopy (XPS), Fourier transform infrared spectroscopy (FTIR), and scanning electron microscopy (SEM) were used to study photodefinition properties. A mechanism based on the diffusion of photoactive compounds is proposed to explain the photo-defined structures.

The crosslinking of the epoxide moieties in poly(decylNB-*co*-epoxideNB) was photoinitiated by acid catalysis. The formulation includes a photoinitiator, a sensitizer and an antioxidant. During exposure to UV light, the sensitizer absorbs energy, creating an excited state (S*). The sensitizer transfers the energy to the photoinitiator.² The photoinitiator then reacts with RH (solvent) to produce H⁺ and R⁻. The epoxide ring opening reaction is initiated by the addition of H⁺ across the bridging oxygen of the epoxide. The reaction continues until the propagating cation reacts with a nucleophile or another polymer chain. The crosslinking reaction of the epoxide groups results in a high

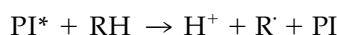
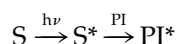
Correspondence to: P. A. Kohl.



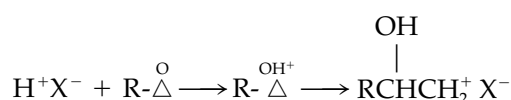
Figure 1 Chemical structure of polynorbornene.

crosslink density of the polymer in the exposed region. The unexposed region dissolves in an appropriate developer, leaving the exposed area intact. The mechanism of photopolymerization is shown below.

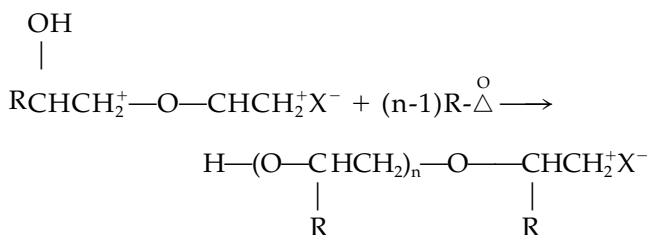
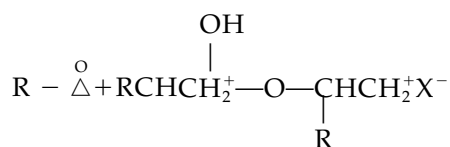
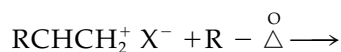
Sensitized decomposition of photoinitiator³:



Initiation:

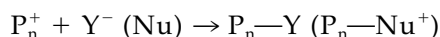


Propagation:

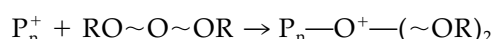


Termination:

a) Termination with the counterion, Y^- , or other nucleophilic compounds (Nu)³:



b) Termination by transfer to the polymer⁴:



P_n^+ : propagating species.

EXPERIMENTAL

The polymers used in this study were 40/60 mol % (40/60) and 70/30 mol % (70/30) poly(decylNB)/poly(epoxideNB) (Promerus LLC, Brecksville, OH), dissolved in anisole. The weight average molecular weight (M_w) and the polydispersity (n) of each formulation were as follows: 40/60 ($M_w = 129,000$; $n = 2.63$); 70/30 ($M_w = 120,000$; $n = 2.11$).

The concentrations of photoactive compounds are reported based on weight percent of dry polymer. Figure 2 shows the chemical structure of the photoinitiator and sensitizer. Several formulations were used in the photodefinition studies: formulation I was 1.0 wt % photoinitiator, 0.5 wt % sensitizer, and 1.5 wt % antioxidant; formulation II was 3.0 wt % photoinitiator, 1.5 wt % sensitizer, and 1.5 wt % antioxidant; and formulation III was 6.0 wt % photoinitiator, 3.0 wt % sensitizer, and 1.5 wt % antioxidant. The chemical structure of the antioxidant is also shown in Figure 2.

Unless otherwise specified, all of the spin coated samples were soft baked at 100°C for 10 min, exposed to 500 mJ/cm² of UV irradiation (365 nm), baked post exposure at 120°C for 20 min, and spray developed for 90 s.

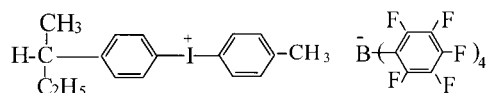
SEM (Hitachi S-3500H) was used to examine the morphology of the via-holes formed in the polymer films coated on the silicon substrates. RBS was used to determine the concentration and depth of the additives in the polymer films. The RBS samples were coated on graphite substrates. He⁺⁺ (2.275 MeV) was used for backscattering. RBS spectra were obtained at a backscattering angle of 160° with the sample normal to the incident ion beam. Additionally, spectra were acquired with the sample in a "rotating random" orientation. This averages the signal over a wide area and prevents beam-induced compositional change. To minimize the polymer film decomposition, the beam spot was moved every 500 nC. Curve fitting was used on the collected data.⁴

XPS was used to determine the atomic composition of the polymer films. Spectra were collected using a Perkin Elmer PHI model 1600 spectrometer. X-rays were generated using a water cooled Al K_α anode operated at 15 V and monochromatized with a quartz crystal. Monochromatic X-rays impinged on the sample at an angle of 45° from the detector axis.

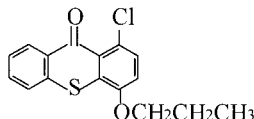
FTIR (Nicolet Magna FTIR 560) was used to monitor the chemical composition in the polymer films. Sixty-four scans with a resolution of 4 cm⁻¹ were collected and averaged to improve the signal-to-noise ratio.

RESULTS AND DISCUSSION

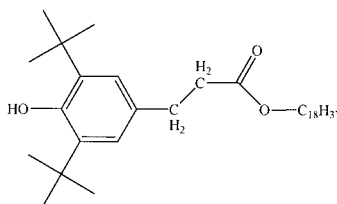
The photodefinition of poly(decylNB-co-epoxideNB) (formulation I) was studied by examining the dimensions of the via-holes formed in the polymer films



Photoinitiator: 4(methylphenyl)-4'-(1-methylethylphenyl) iodonium tetrakis (pentafluorophenyl) borate (Rhodorsil 2704)



Sensitizer: 1-chloro-4-propoxy-9H-thioxanthen-9-one (CPTX)



Antioxidant: octadecyl 3,5 di-tert-butyl-4-hydroxycinnamate (Irganox™ 1076)

Figure 2 Chemical structures of photoinitiator, sensitizer and antioxidant.

upon exposure, bake and development. The mask used in the photodefinition study had opaque circles with a radius of $300\ \mu\text{m}$. The unexposed area was not crosslinked and was dissolved in developer. This resulted in the formation of via-holes in the polymer film after development (Fig. 3). The sidewall profile and diameter of the via-holes were examined. Of particular interest was the formation of a lip at the top of the via-holes and of residue (or "foot") at the bottom (shown with the dashed lines in Fig. 3). The average diameter of a via-hole and size of lip and foot are shown at A, B, and C of Figure 3, respectively. It was

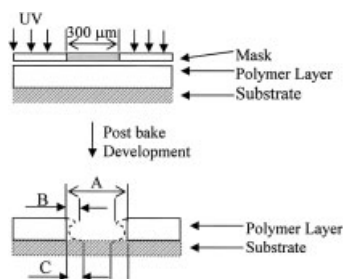
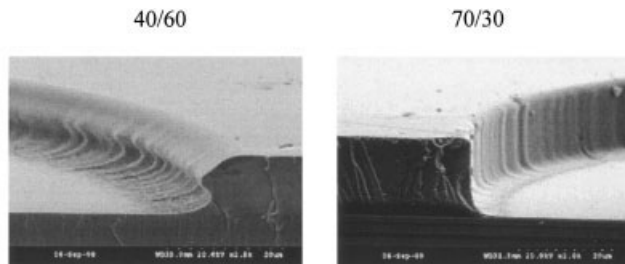


Figure 3 Illustration of via-hole formed in polymer film.

found that the sidewall profile and the via-hole size varied with copolymer composition, concentration of photoactive compounds, and processing conditions, including exposure dose and post bake temperature. The relationships are described in detail below.

Figure 4 shows the sidewall profiles of via-holes opened in 40/60 and 70/30 polymer films (Formulation II). The via-holes opened in 40/60 and 70/30 polymer films showed very different sidewall profiles. The maximum diameter (A) was less than $300\ \mu\text{m}$ in both cases. There was a lip at the top and residue at the bottom of the via-hole opened in the 40/60 polymer film. The lip and residue, which extended into the via-hole opening, were about $12.93\ \mu\text{m}$ and $17.29\ \mu\text{m}$ in size, respectively. The via-hole opened in the 70/30 polymer had a vertical sidewall profile with no lip at the top, and the residue at the bottom was about $6.48\ \mu\text{m}$ in size. In addition, the via-hole opened in the 40/60 film had a smaller diameter ($285.04 \pm 0.60\ \mu\text{m}$) than the via-hole opened in the 70/30 film ($294.94 \pm 1.09\ \mu\text{m}$).

The 40/60 polymer was used to examine the photodefinition properties as a function of concentration of photoactive compounds and processing conditions.



Polymer	A (μm)	B (μm)	C (μm)
40/60	285.04 ± 0.60	12.93 ± 1.16	17.29 ± 3.13
70/30	294.94 ± 1.09	0	6.48 ± 0.93

Figure 4 SEM pictures of the via-hole opened in 40/60 and 70/30 polymer films (formulation II).

Figure 5 shows the sidewall profiles of the via-holes opened in the 40/60 polymer film with (a) 1 wt % photoinitiator, 0.5 wt % sensitizer (formulation I) and (b) 3 wt % photoinitiator, 1.5 wt % sensitizer (formulation II). There was no lip or residue, as shown in Figure 5(a). The via-hole had a vertical sidewall profile with a diameter of 294.80 ± 0.92 μm. However, the lip extended 12.93 μm and residue extended 17.29 μm into the via-hole in the polymer film with a high concentration of photoactive compounds.

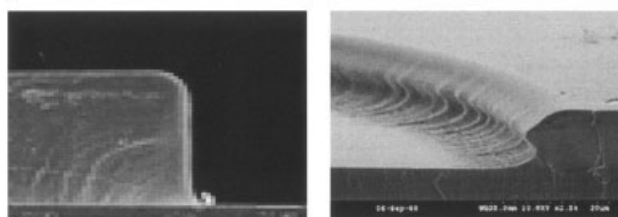
Figure 6 shows SEM pictures and the sizes of the via-holes opened in the 40/60 polymer films (formulation II) exposed to 200, 500, and 1000 mJ/cm² doses. All if the via-holes opened in the 40/60 polymer films showed lips at the top and some residue at the bottom. The lip was larger with increasing exposure dose. The size of the lip increased from about 6.34 μm to 16.69 μm, and the size of residue increased from 11.00 μm to 34.65 μm when the exposure dose increased from 200 mJ/cm² to 1000 mJ/cm². The radii of the vias de-

creased from 295.52 ± 0.38 μm to 278.50 ± 1.27 μm when the exposure dose increased from 200 mJ/cm² to 1000 mJ/cm².

Figure 7 shows the SEM pictures and the dimension sizes of the via-holes opened in the 40/60 polymer films (formulation II) processed at post-exposure bake temperatures of 100 and 120°C. The SEM pictures show that the via-hole opened in the film post-exposure baked at 100°C had a smaller lip (≈6.79 μm) and less residue (≈15.00 μm) than the via-hole opened in the film post-exposure baked at 120°C. In addition, the via-hole opened in the film post-exposure baked at 100°C had a larger diameter (290.88 ± 0.80 μm) than the via-hole opened in the film post-exposure baked at 120°C (285.04 ± 0.60 μm).

These results show that crosslinking occurs in the geometric shadow and is exacerbated by high epoxy concentration, high exposure dose, high post-exposure bake temperature, and high concentration of photoactive compounds. There was a lip at the top of the

(a) Formulation I (b) Formulation II



Photoinitiator Conc.	A (μm)	B (μm)	C (μm)
3 %	285.04 ± 0.60	12.93 ± 1.16	17.29 ± 3.13
1 %	294.80 ± 0.92	0	4.52 ± 0.87

Figure 5 SEM pictures of the via-holes opened in 40/60 films with (a) 1 wt % photoinitiator and 0.5 wt % sensitizer (formulation I) and (b) 3 wt % photoinitiator and 1.5 wt % sensitizer (formulation II).

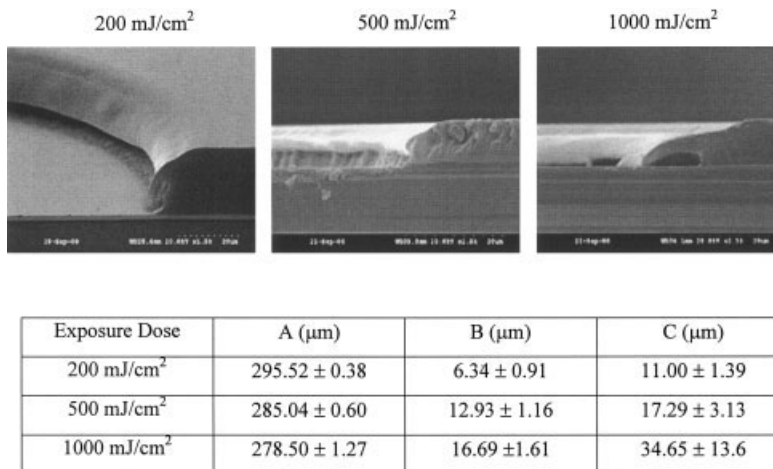


Figure 6 SEM pictures of the via-holes opened in 40/60 polymer films (formulation II) exposed to 200, 500, and 1000 mJ/cm² doses.

via-hole and some residue at the bottom under certain conditions. A possible reason for the crosslinking reaction in the unexposed area is the migration of photoactive compounds from the exposed area. RBS, XPS, FTIR, and SEM were used to investigate the transport of the photoactive compounds into the unexposed area.

The lip at the top of the via-hole may result from higher concentrations of photoactive compounds, which moved into the unexposed area and caused a higher level of crosslinking at the top of the via-hole. Thus, there is interest in determining the concentration of photoactive compounds as a function of depth in the films. The changes in the concentration profiles for the photoactive compounds with exposure and post-exposure bake are important. RBS spectra were obtained on both the spin coated (and soft baked) and post-exposure baked single-layer 40/60 polymer films (formulation III). The polymer was spin coated on a

graphite substrate and soft baked at 100°C for 10 min. A duplicated spin coated sample was taken through the exposure step (500 mJ/cm² dose) and post-exposure baked at 120°C for 20 min. The thickness of the polymer film was about 2.5 μm. The atoms of interest included S and Cl, which are contained in the sensitizer, B and F, which are contained in the anion part of the photoinitiator, and I, which is contained in the cation part of the photoinitiator. The corresponding energy channel and the detection uncertainties for these atoms are listed in Table I.

The atomic percent of the atoms was calculated from the RBS spectra. Cl and S were difficult to distinguish from each other because they are too close in atomic mass. Thus, the sum of their atomic percent is reported as the tracer of the sensitizer. Boron was not analyzed in this study due to its low atomic mass. The expected atomic percent values for the atoms were calculated based on the polymer formulation. The

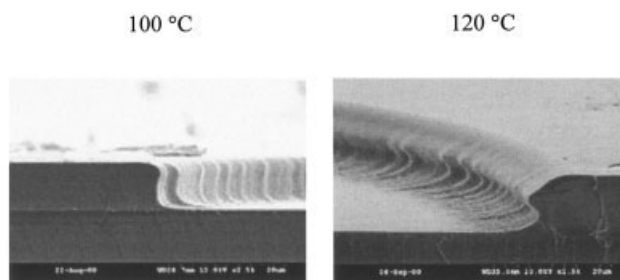


Figure 7 SEM pictures of the via-holes opened in 40/60 polymer films (formulation II) post-exposure baked at 100°C and 120°C.

TABLE I
Detection Uncertainties for Surface Atoms
Detected in RBS¹⁴

Material	Elements	Uncertainty (%)
Polymer	C	± 3
	I	± 0.01
	F	± 0.07
Photoinitiator	B	—
	S	± 0.02
	Cl	± 0.02

depth profiles for the soft baked and post-exposure baked samples are shown in Figure 8. Table II gives a summary of the atomic concentrations broken down by depth.

In the soft baked 40/60 polymer film, the distributions of I and F were relatively uniform with depth. The atomic concentrations of I and F were 0.030 and 0.5 at %, respectively, which matched the expected values within experimental error. The sum of the atomic percentages of S and Cl was nearly constant with depth (0.09 at %). The absolute concentrations of S and Cl were close to the values calculated from the formulations and well within the uncertainty for light elements. The data show that after soft bake, the sensitizer (Cl and S) and photoinitiator (I and F) were uniformly distributed throughout the film at approximately the formulated concentrations.

In the post-exposure baked 40/60 polymer film, F was uniformly distributed throughout the film. The atomic percent of I was significantly lower than in the soft baked sample. The sum of the atomic percents of S and Cl was higher near the surface than in the bulk. Thus, the relative distribution shows an accumulation of sensitizer and anion of photoinitiator at the surface and a depletion of I, the initiator cation, from the film.

Some general conclusions can be drawn based on the RBS results. First, the atomic percents of all atoms

were consistent with the formulated values in the soft baked sample (within measurement uncertainties). Second, the concentration of I, the initiator cation, was much lower after post-exposure baking of the films. In addition, the concentration of I at the surface was about 30% higher than that in the bulk in the post-exposure baked samples. Third, the changes in concentration are due to the transport of sensitizer and initiator ions and not to systematic errors in measurement (i.e. uniform off-set in all data), since some values increase and some decrease.

These results suggest that the sensitizer CPTX has a higher concentration on the surface for the exposed and post-exposure baked samples, which most likely leads to a higher concentration of photogenerated acid at the surface.

An important question is the relationship between the sensitizer and photoinitiator diffusion and the lip shown in Figures 4–7. The lip occurs in the geometric shadow of the UV exposure. It is necessary to determine whether the photoactive compounds migrate to the unexposed area and thus cause the crosslinking reaction in the geometric shadow. A two-layer structure was fabricated to investigate the movement of the photoactive compounds. A first layer of formulated polymer (formulation III) ($\approx 2 \mu\text{m}$) was spin coated, soft baked at 100°C for 10 min and exposed at $150 \text{ mJ}/\text{cm}^2$. It was post-exposure baked at 100°C for 5 min. This procedure gave the polymer film a degree of crosslinking to avoid swelling in the second coating. An unformulated polymer layer (containing no photoactive compounds) was then coated on top of the first layer. The thickness of the unformulated polymer layer was about $1 \mu\text{m}$. The sample was soft baked at 100°C for 10 min to evaporate the solvent from the unformulated polymer layer. A duplicate sample was exposed to a dose of $500 \text{ mJ}/\text{cm}^2$ and post-exposure baked at 120°C for 20 min to simulate the photoinitiator and sensitizer migration process. The RBS spectra

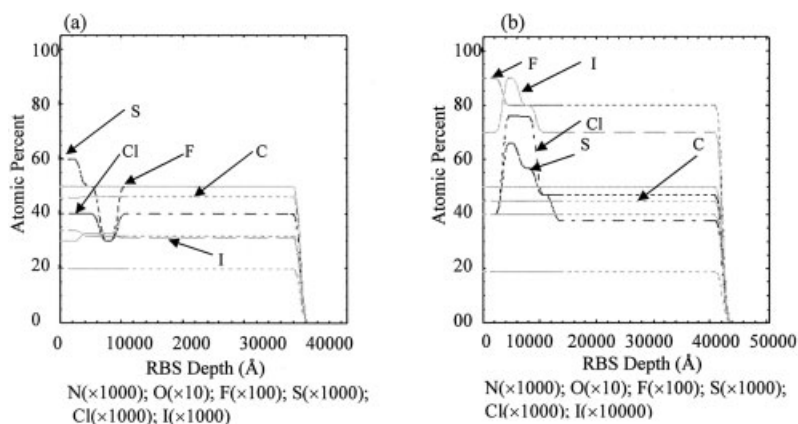


Figure 8 Depth profiles of the atomic percent for (a) soft baked and (b) post-exposure baked 40/60 polymer films (formulation III).

TABLE II
Atomic Percent with Depth for Soft Baked and Post-Exposure Baked 40/60 Polymer Films

Sample	T_{RBS} (Å)	Atomic percent			
		C	F	I	S + Cl
Formulated value	All depth	50.0	0.8	0.043	0.14
SB 40/60	< 3000	45.8	0.5	0.030	0.10
	3000–6000	46.0	0.5	0.033	0.09
	6000–9000	46.0	0.5	0.033	0.06
	> 9000	46.0	0.5	0.031	0.09
PEB 40/60	< 3000	44.8	0.9	0.007	0.08
	3000–6000	44.9	0.8	0.009	0.14
	6000–9000	44.9	0.8	0.008	0.12
	9000–12000	44.9	0.8	0.007	0.10
	> 12000	44.9	0.8	0.007	0.08

were obtained for both soft baked and post-exposure baked two-layer 40/60 samples. The atomic concentrations are listed in Table III. Both soft baked and post-exposure baked two-layer structures of the 40/60 polymer films showed the presence of S and Cl in the top polymer layer, without added formulation. The atomic concentration of S and Cl was 0.160% in the soft baked sample and 0.115% in the post-exposure baked sample. The results show that the sensitizer in the formulated polymer layer diffused into the top, unformulated polymer layer during the soft bake step and then moved out of the polymer film during the post-exposure bake. The RBS spectra also demonstrate the existence of I in the top, unformulated polymer, indicating diffusion of the iodoaromatic compound, Ar—I, from the bottom, formulated polymer layer. The atomic percent of I was 0.001% in both the soft baked and the post-exposure baked samples. However, the identification of F was not possible in this experiment because of its low sensitivity. XPS was used to analyze the surface of the polymer for the presence of F in the top, unformulated polymer film. Analyses of both soft baked and post-exposure baked two-layer 40/60 polymer films were performed. The XPS spectra are shown in Figure 9. The XPS spectra shows the 1s peak of the F atom in the top, unformulated polymer layer of the post-exposure baked two-layer structure. The XPS spectra did not show the presence of F in the soft baked two-layer structure. This shows that the anion part of the photoinitiator diffused into the top, unformulated polymer layer

from the bottom, formulated polymer film during the post-exposure bake step.

The results from RBS and XPS show that sensitizer and photoinitiator can vertically diffuse from the exposed and baked polymer into the unexposed polymer layer. The presence of sensitizer and photoinitiator creates the opportunity for crosslinking in the unexposed area. A set of test samples was fabricated to mimic diffusion and crosslinking in the horizontal (in-plane) direction. Attenuated total reflection (ATR) FTIR was used to monitor the crosslinking reaction in the top, unformulated polymer layer for both soft baked and post-exposure baked two-layer 40/60 samples. The thickness of the bottom, formulated polymer layer was about 2 μm , and the thickness of the top, unformulated polymer layer was about 1 μm . Only the top, unformulated polymer layer was analyzed by ATR FTIR because its penetration depth is about 0.4 μm . The spectra of the soft baked and post-exposure baked samples are shown in Figure 10. The ATR spectra show the characteristic peak of the C—O—C stretch for epoxy rings at 844 cm^{-1} for both samples. The peak height decreased in the post-exposure baked sample compared to the soft baked sample. About 30% of the epoxide groups in the top, unformulated

TABLE III
Atomic Percent of Elements in Two-Layer Structure Obtained from RBS

Sample	RBS depth (Å)	Atomic percent		
		C	S + Cl	I
SB 40/60	Bulk	45.4	0.160	0.001
PEB 40/60	Bulk	45.6	0.115	0.001

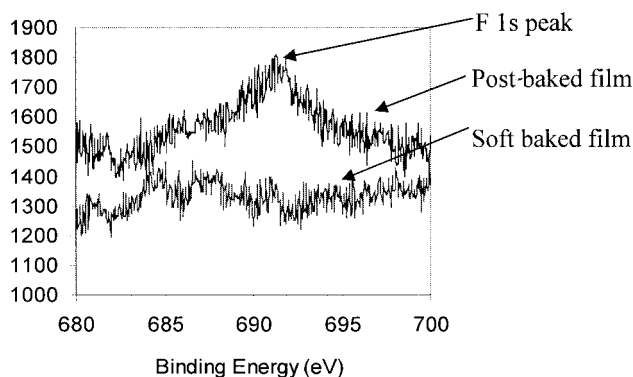


Figure 9 XPS spectra of soft baked and post-exposure baked two-layer structure of 40/60 polymer.

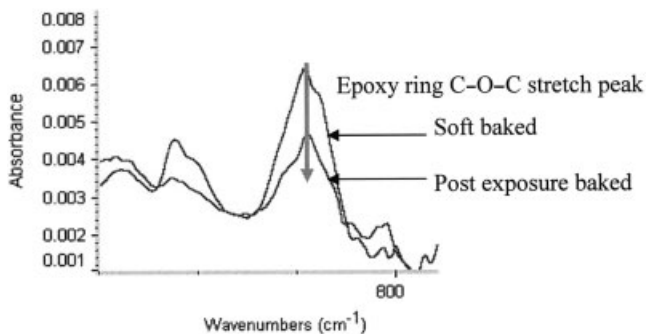


Figure 10 ATR spectra of soft baked and post-exposure baked two-layer structure of 40/60 polymer.

pure polymer layer reacted after the exposure and the post-exposure bake. The crosslinking reaction was caused by the photoactive compounds diffusing from the formulated layer.

The vertical (through-plane) diffusion of photoactive compounds into the unformulated polymer causes crosslinking in the top, unformulated polymer film. The change in solubility of the polymer film as a result of the crosslinking reaction was investigated. An SEM experiment was carried out on the two-layer structure using the 40/60 polymer. The formulated polymer (formulation III) was first spin coated on a Si wafer and then soft baked at 100°C for 10 min. The thickness of the formulated polymer layer was about 10 μm. The formulated polymer film was not exposed to UV light. Unformulated polymer was then coated on top of the first layer and soft baked at 100°C for 10 min. The two-layered structure was exposed to a UV dose of 500 mJ/cm² through a mask, and post-exposure baked at 120°C for 20 min. The polymer film was then developed to reveal the exposure patterns. A cross-sectional SEM of the pattern is shown in Figure 11.

The pattern formed in the top, unformulated polymer layer shows that some crosslinking occurred in the unformulated layer due to diffusion from the formulated region. However, the lip at the top of the via-hole and the smaller radius of the via-hole was likely caused by in-plane diffusion of the photoactive compound from the exposed area to the unexposed area.

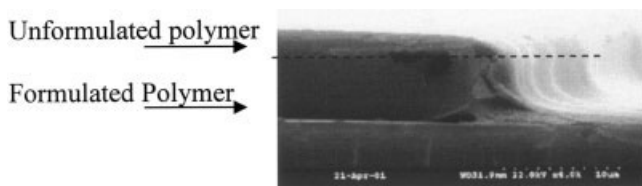


Figure 11 SEM picture of the pattern formed on the two-layer structure of 40/60 polymer.

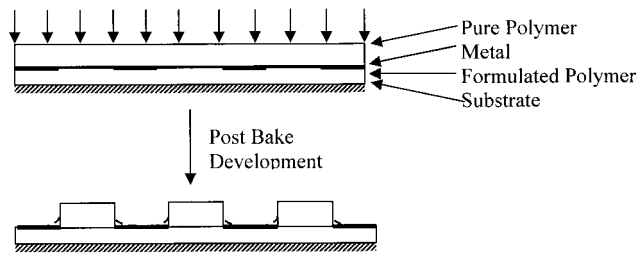


Figure 12 Illustration of three-layer structure.

A three-layer structure with a metal layer between formulated polymer and unformulated polymer was built to test the in-plane diffusion of photoactive compounds. Figure 12 shows the three-layer structure. For the three-layer structure, the formulated polymer (formulation III) was spin coated on the Si wafer and soft baked at 100°C for 10 min. A thin layer of metal (Ti) was sputtered on the top of the polymer film, and a pattern was created using photolithography and chemical etching of the Ti. The thickness of the Ti metal layer was about 1000 Å. A layer of the unformulated polymer was coated on the top of the metal layer. The sample was then irradiated with UV light of 500 mJ/cm², post baked, and developed. If unformulated, un-crosslinked polymer remained on the top of the metal, it would dissolve in the developer. Horizontal (in-plane) motion of the photoactive compounds into regions above the metal caused crosslinking there. Normally, the metal would serve as a barrier to the through-plane diffusion of the photoactive compounds (shown in Fig. 12). The SEM picture of the pattern created in the three-layer structure of 40/60 polymer (Fig. 13) shows a tail in the unformulated polymer on top of the metal. This shows that the photoactive compounds first diffused into the pure polymer film vertically (through-plane) and then horizontally (in-plane).

Discussion

The spatial resolution of the photodefined polymer is critical to successful implementation, while specific

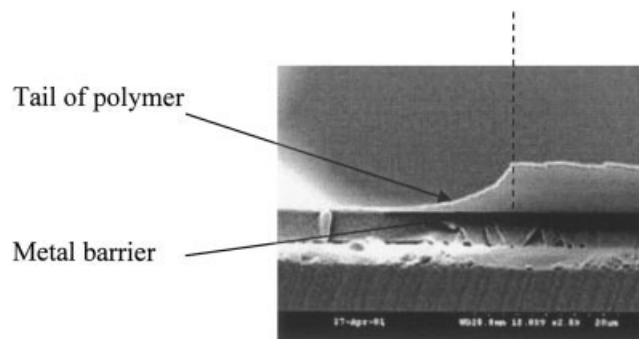


Figure 13 SEM picture of pattern formed in three-layer structure of 40/60 polymer.

conditions can be found for high resolution photopatterning. The transport of the photoactive compound through a single-layer formulated layer was demonstrated by RBS analysis. The concentrations of I, S, and Cl were higher at the surface and depleted from the bulk in the post-exposure baked films. The relatively high concentrations of I, S, and Cl on the surface of the single layer polymer film may be attributed to the diffusion of small molecules during the post-exposure bake. This process may be explained by the free volume theory. The evaporation of the solvent generates transient free volume in the polymer film during the soft bake and post-exposure bake steps.⁵ The bake temperatures were below the glass transition temperature of the polymer film. Glassy polymers do not respond immediately to a change in their equilibrium state.⁶ Thus, the elimination of free volume after solvent evaporation is not instantaneous, and small molecules may diffuse through the channels created by the free volume in the polymer film. The work by Hofmann et al. indicates that the diffusion of small molecules in stiff-chain polyimides is based on jumps through temporary channels between adjacent voids in the polymer matrix.⁷ In addition, simulations have shown that the free surface region may have a lower density and higher free volume compared to the bulk,^{8,9} contributing to the higher concentrations of small molecules on the surface. The calculation and simulation results by Hariharan et al. suggests a purely entropic effect that the smaller chains preferentially migrate to the interface in order to enable the system to reach a state of maximum possible entropy at equilibrium.¹⁰ Janarthanan et al. confirmed the transport of small molecules to the polymer surface.¹¹

The lower concentrations of I, S, and Cl in the single-layer polymer are due to the volatility of the small molecules during the post-exposure bake. Chinwalla¹² et al. confirmed that the sensitizer migrates out of the polymer film at temperatures below 120°C.

The RBS and XPS results for the two-layer structure involving unformulated-on-formulated polymer showed that I, F, S, and Cl atoms were transported from the bottom to the top layer. This shows that the sensitizer and the photoinitiator migrate to the top, unformulated polymer layer from the bottom, formulated polymer layer.

The ATR FTIR results demonstrate that the transported photochemicals can initiate epoxide ring opening in the unformulated polymer layer even though that layer did not originally contain photoactive compounds. Further, it was shown that the photoactive compounds could laterally migrate into the unexposed region from the three-layer structure and cause epoxide ring opening in that region.

On the basis of these results, a reaction sequence can be constructed. The photopolymerization of the polynorbornene polymer is initiated by photogener-

ated acid. The photogenerated acid moves horizontally and/or vertically into the unexposed area. Crosslinking occurs in the unexposed area, reducing the size of the via-hole. The concentration of the sensitizer tends to be higher in the top surface of the formulated polymer layer, possibly due to the increased free volume as the solvent evaporates. At higher post-exposure bake temperatures, the rate of acid diffusion is increased, further reducing the via-hole size. When the polymer film is exposed to a higher exposure dose, more acid is generated, inducing a higher crosslink density.

In summary, a higher epoxide/NB content, exposure dose, post-exposure bake temperature, or photoactive compound concentration results in a higher crosslink density in the unexposed area due to acid diffusion. This can lead to poor photodefinition of the polymer.

CONCLUSIONS

Polymer formulations and processing conditions have been found to produce highly vertical sidewall structures. The photodefinition properties of poly(decylNB-co-epoxideNB) were affected by the copolymer composition, the concentration of photoactive compounds and the processing conditions. The diameter of the opened via-holes tends to be smaller than that of the mask, and a lip can form at the top of the via-hole. These defects become more obvious when the polymer contains higher epoxy content or photoactive compound concentration, or when it is prepared at higher bake temperatures. Migration of photoactive compounds was observed. The migration takes place in both vertical and horizontal directions and can degrade the spatial resolution of the copolymer.

References

1. Tummala, R. R.; Rymaszewski, E. J.; Klopfenstein, A. G. *Microelectronics Packaging Handbook*; Kluwer Academic Publishers: , 1999.
2. Fouassier, J. P. *Photoinitiation Photopolymerization and Photocuring*; Rapra Technology: Shawbury, UK, 1998.
3. Crivello, J. V. *Adv in Polym Sci* 1986, 62, 1.
4. Fouassier, J.; Babek, J. *Radiation Curing in Polymer Science and Technology*; Elsevier Applied Science: New York, 1993.
5. Croffie, E.; Cheng, M.; Neureuther, A. *J of Vacuum Sci Tech* 1999, B17(6) 3339.
6. Pain, L.; LeCornec, C.; Rosilio, C.; Paniez, P. J. *Microelectronic Engin* 1996, 30, 271.
7. Hofmann, D.; Fritz, L.; Ulbrich, J.; Paul, D. *Comp and Theor Polym Sci* 2000, 10, 419.
8. Mansfield, K. F.; Theodorou, D. N. *Macromolecules* 1991, 24, 6283.
9. Mayes, A. *Macromolecules* 1994, 27, 3114.
10. Hariharan, A.; Kumar, S. K. *Macromolecules* 1990, 23, 3584.
11. Janarthanan, V.; Stein, R. S.; Garrett, P. D. *J Polym Sci Part B: Polym Phys* 1993, 31, 1995.
12. Chinwalla, P. Ph.D. Dissertation, Georgia Institute of Technology, 2001.